SLAS Discovery
2020, Vol. 25(1) 95–103


DOI: 10.1177/2472555219860779
journals.sagepub.com/home/jbx


A Sensitive and Selective Immunoassay for the Quantitation of Serum Latent Myostatin after In Vivo Administration of SRK-015, a Selective Inhibitor of Myostatin Activation

Shaun M. Cote[1], Justin Jackson[1], Michelle Pirruccello-Straub[1], Gregory J. Carven[1], and Stefan Wawersik[1]

Abstract

Myostatin, a member of the transforming growth factor β (TGFβ) superfamily, is a key regulator of skeletal muscle mass and a therapeutic target for muscle wasting diseases. We developed a human monoclonal antibody, SRK-015, that selectively binds to and inhibits proteolytic processing of myostatin precursors, thereby preventing growth factor release from the latent complex. As a consequence of antibody binding, latent myostatin accumulates in the circulation of animals treated with SRK-015 or closely related antibodies, suggesting that quantitation of latent myostatin in serum may serve as a biomarker for target engagement. To accurately measure SRK-015 target engagement, we developed a sensitive plate-based electrochemiluminescent immunoassay to quantitate latent myostatin in serum samples. The assay selectively recognizes latent myostatin without cross-reactivity to promyostatin, mature myostatin, or closely related members of the TGFβ superfamily. To enable use of the assay in samples from animals dosed with SRK-015, we incorporated a low-pH step that dissociates SRK-015 from latent myostatin, improving drug tolerance of the assay. The assay meets inter- and intra-assay accuracy and precision acceptance criteria, and it has a lower limit of quantitation (LLOQ) of 10 ng/mL. We then tested serum samples from a pharmacology study in cynomolgus monkeys treated with SRK-015. Serum latent myostatin increases after treatment with SRK-015, reaches a dose-dependent plateau approximately 20 days after dosing, and trends back toward baseline after cessation of antibody dosing. Taken together, these data suggest that this assay can be used to accurately measure levels of the primary circulating form of myostatin in population-based or pharmacodynamic studies.

Keywords

myostatin, immunoassay, cynomolgus monkey

Introduction

The transforming growth factor beta (TGFβ) superfamily protein myostatin [growth differentiation factor 8 (GDF8)] is a potent negative regulator of skeletal muscle mass. Myostatin is expressed primarily in skeletal muscle,[1] with low levels of messenger RNA (mRNA) reported in adipose[2] and cardiac[3] tissues. Mutations that attenuate myostatin signaling lead to a hypermuscular phenotype in multiple species,[4–9] and, conversely, genetic overexpression in rodents induces muscle wasting and fat loss.[10] As a consequence of its impact on muscle mass, myostatin is an attractive drug target for diseases involving muscle atrophy, and agents that target the myostatin signaling pathway have entered the clinic for such disorders.

Myostatin is initially expressed as promyostatin, a pro-protein in which the active C-terminal growth factor is held in a dimeric latent complex through association with a large prodomain. Release of the mature growth factor from the

[1]Scholar Rock, Inc., Cambridge, MA, USA

Received Apr 1, 2019, and in revised form May 10, 2019. Accepted for publication Jun 5, 2019.

Supplemental material is available online with this article.

Corresponding Author:
Shaun M. Cote, Scholar Rock, 620 Memorial Drive, Cambridge, MA 02139, USA.
Email: scote@scholarrock.com

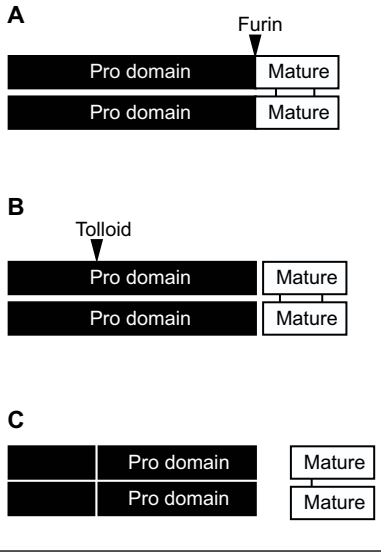

D

Antibody	Relative Binding Affinity Pro	Latent	Mature
SRK-015	++	++	-
GDF8_013	+	+	-
GDF8_020	+	-	-
GDF8_021	+	-	-
GDF8_024	+	-	-
GDF8_029	++	++	-
GDF8_039	+	++	-
GDF8_040	++	+	-
GDF8_050	+	-	-
GDF8_062	-	+	-
GDF8_084	-	+	-
GDF8_090	+	+	-
SR8-C1	-	++	+
RK22	+	+	+
RK35	+	+	+

Figure 1. Processing of the promyostatin complex into the active growth factor. (**A**) Promyostatin is cleaved by a furin protease to generate (**B**) latent myostatin. (**C**) An additional cleavage by a tolloid protease allows subsequent release of the active growth factor. (**D**) Summary of the relative binding affinities of antimyostatin antibodies for the pro-, latent, and mature myostatin forms.

unprocessed precursor is regulated through two discrete protease cleavage events (**Fig. 1**): First, promyostatin is cleaved at a conserved RXXR motif between the prodomain and mature growth factor by proprotein convertases such as furin/PACE3 (paired basic amino acid cleaving enzyme 3) or PCSK5 (proprotein convertase subtilisin/kexin type 5).[10–12] This initial cleavage produces latent myostatin, an inactive complex in which the prodomains remain associated with the growth factor.[13] A second prodomain cleavage by members of the BMP/tolloid family, such as TLL2 (tolloid-like protein 2) or BMP1 (bone morphogenetic protein 1), activates latent myostatin by releasing the mature growth factor from the latent complex, allowing it to bind to ActRIIB (activin receptor type IIB) receptors, and thereby activating downstream signaling.[11–14]

We recently described the identification and characterization of SRK-015, a monoclonal antibody that inhibits the tolloid-mediated proteolysis of latent myostatin.[15] SRK-015 binds pro- and latent myostatin but does not bind the mature growth factor or any forms of GDF11, myostatin's closest paralog.[15] Furthermore, SRK-015 shows no binding to closely related TGFβ family members activin A, bone morphogenic protein 9 (BMP9), BMP10, and TGFβ1.[15] Analogs of SRK-015 have been shown to increase muscle mass and function in healthy mice and in mice with muscle atrophy caused by dexamethasone treatment[15] or by genetic mutations in the *Smn1* gene, which encodes the survival motor neuron protein.[16] Using semiquantitative Western blots, we have previously shown that latent myostatin is the primary form of the protein detectable in serum or plasma, and that dosing mice with analogs of SRK-015 leads to significant accumulation of circulating latent myostatin.[15] Thus, measuring this pool of latent myostatin may provide insight into the kinetics of target engagement and saturation in SRK-015-treated subjects. In addition, when paired with well-characterized protocols for evaluating muscle function and basic motor skills,[17–20] accurate measurement of latent myostatin may inform dose selection and frequency for clinical trials that aim to evaluate the efficacy of this inhibitor of myostatin activation.

Circulating myostatin levels have been measured by enzyme-linked immunosorbent assay (ELISA)-based assays directed at the mature myostatin growth factor.[21–26] These assays, however, require acid dissociation of the growth factor from the latent complex, with latent myostatin levels inferred from the difference between acid-treated and non-acid-treated serum. Furthermore, the high amino acid conservation between myostatin, GDF11, and activin A[27,28] raises the possibility of cross-reactivity in growth factor–targeted ELISAs. For these reasons, specific, quantitative pro- or latent myostatin measurement has thus far been achieved only by mass spectrometry–based methods.[29–32]

Using antibodies directed at the myostatin prodomain, we previously developed a Western blot–based method to quantify relative changes in latent myostatin expression.[15] Because Western blots are semiquantitative and low-throughput, however, we have subsequently developed a sensitive, robust, and highly selective plate-based ligand binding assay to directly measure latent myostatin. This assay, which we describe here, was developed using best practices and was qualified using a fit-for-purpose qualification strategy.[33,34] We also present data generated using our assay to evaluate latent myostatin accumulation in SRK-015-treated samples from a pharmacology study in cynomolgus monkeys.

Materials and Methods

Antibodies and Reagents

Several antimyostatin antibodies were identified from phage display campaigns using the recombinant promyostatin or latent myostatin complexes as input antigens (SRK-015, GDF8_013, GDF8_020, GDF8_021, GDF8_024, GDF8_029, GDF8_039, GDF8_040, GDF8_050, GDF8_062, GDF8_084, and GDF8_090).[15] The latent myostatin inhibitor SRK-015 is a fully human immunoglobulin G4 (IgG4) monoclonal antibody whose discovery and characterization have been previously described.[15,16] The remainder of the antibodies identified from the phage display campaign exhibited the binding profiles shown in **Figure 1D**. Additional antimyostatin antibodies, not discovered at Scholar Rock, were used in this study. These antibodies, SR8-C1,[11,35] RK22,[21,36] and RK35,[21,37] exhibit binding only to latent and mature myostatin. All antibodies were cloned as human IgG4 monoclonal antibodies and were produced using the Expi293 polyethylenimine (PEI) expression system, following the manufacturer's protocol (Thermo Fisher Scientific, Waltham, MA). The antibodies were purified from the supernatant using protein A resin, followed by polishing over a size exclusion column.

Antibodies were labeled with biotin (EZ-Link Sulfo-NHS-Biotin, cat. no. 21217; Thermo Fisher Scientific) or ruthenium (MSD Gold Sulfo-tag NHS-Ester, cat. no. R91AO; Meso Scale Discovery, Rockville, MD) following the manufacturer's protocols.

Promyostatin was generated using the Expi293 PEI expression system as previously described.[15] After expression, to generate a pool of pure promyostatin, the protein material was further purified over an antilatent myostatin affinity column with the antibody SR8-C1 to remove latent myostatin from the protein sample (**Suppl. Fig. 1A**).

Latent myostatin was prepared by proteolytic cleavage of promyostatin with furin (cat. no. P8077S; New England Biolabs, Ipswich, MA). A 2 mg/mL aliquot of promyostatin was diluted into the cleavage buffer (100 mM HEPES, 0.001% Brij-35, 0.1 mM $CaCl_2$, and 0.1 μM $ZnCl_2$). Furin was added at a concentration of 10 units per nmol, and the reaction was incubated for 4 h at 30 °C. An additional 10 units per nmol of furin was then added to the reaction and incubated overnight at 30 °C. Following cleavage, resulting latent myostatin was purified on an affinity column conjugated with an anti-promyostatin antibody (GDF8_021) equilibrated with HEPES buffer to remove residual promyostatin from the protein sample (**Suppl. Fig. 1B**).

Generation of Myostatin-Depleted Serum

Prior to the generation of standards and controls, pooled normal cynomolgus monkey serum (BioIVT, Westbury, NY) was depleted of endogenous myostatin using an affinity column prepared through amine coupling of antibody RK22 directly on functionalized resin. Briefly, a 100 μL volume of depletion column resin was added to 25 mL of normal cynomolgus monkey serum and was incubated overnight at 4 °C with rotation. The resin was then separated from serum by centrifugation at 1000×g for 5 min, followed by two additional 4 h incubations with 100 μL resin, with centrifugation after each incubation. Depleted serum was assayed to confirm removal of myostatin using the assay protocol described below.

Latent Myostatin Quantitative Immunoassay

Small-spot streptavidin Gold Assay plates (cat. no. L45SA; Meso Scale Discovery) were blocked with the assay diluent [2.5% bovine serum albumin (BSA) in tris-buffered saline, pH 7.4, with 0.1% Tween-20] for 1 h at room temperature (RT). The blocking solution was aspirated, and the biotinylated coating antibody SR8-C1 was added to the plate and incubated for 1 h at RT, followed by a wash step. This and all subsequent wash steps consisted of three washes in TBST (a mixture of tris-buffered saline and Tween-20). Samples, standards, and controls were diluted to the minimum required dilution (MRD) of 1:100 or further in either the assay diluent or a low-pH diluent (2.5% BSA in 20 mM citrate, pH 4.0, 150 mM sodium chloride, and 0.1% Tween-20). Standards, controls, and samples were applied to the plate and incubated for 2 h at RT, followed by a wash step. A solution of the ruthenium-tagged detection antibody (coded as GDF8_090) was added to the plate and incubated for 1 h at RT, followed by a wash step. Read Buffer T (cat. no. R92TC; Meso Scale Discovery) was diluted to 2× with water, added to the plate, and immediately read on a MESO QuickPlex SQ 120 instrument (cat. no. AI0AA-0; Meso Scale Discovery).

To determine the matrix effect and MRD for the assay, a standard curve was prepared in assay buffer (2.5% BSA in 20 mM citrate, pH 4.0, 150 mM sodium chloride, and 0.1% Tween-20) with 0%, 1%, or 10% myostatin-depleted cynomolgus serum. These standard curves were assayed using the above protocol.

For initial identification of antibody pairs that optimally detect latent myostatin, the concentration of each antimyostatin antibody, used as either the capture or detection reagent, was 1 μg/mL. In the qualified assay format, the concentration of SR8-C1–biotin was 5 μg/mL, and the concentration of GDF8_090–ruthenium was 0.5 μg/mL. The LLOQ was established at the lowest concentration of latent myostatin that gave a signal approximately twofold greater than the background signal, recovered within 75–125% of the nominal concentration, and had a coefficient of variation (CV) of <25% and a total error of <30%. The assay range of quantitation is 10 to 16,667 ng/mL in neat serum (0.1 to 166.7 ng/mL in 10% serum). All curves were fitted to a five-parameter logistic function with $1/y^2$ weighting.

Assay Qualification

For the qualification, the assay was performed as described above with the following changes based on the specific analysis. For dilutional linearity, a control containing latent myostatin was prepared at a nominal concentration of 40 µg/mL and diluted in series to up to 1000-fold. For stability assessments, three sets of the high and low controls were assayed after different treatments: One set was subjected to repeated freeze–thaw cycles consisting of a 1 h incubation at −80 °C, followed by 1 h incubation at RT. A second set of controls was incubated for 4 h at RT, and the third set was incubated overnight at 2–8 °C.

Determination of Antibody pH Sensitivity

The pH sensitivity of antimyostatin antibody binding to latent myostatin was determined by biolayer interferometry using a ForteBio Octet QK^E instrument (ForteBio, Fremont, CA). First, streptavidin-conjugated sensors were pre-wet for 10 min and then equilibrated for 1 min in kinetics buffer (1× PBS, 0.002% Tween-20, and 0.1% albumin). Next, 75 nM of biotinylated human latent myostatin was immobilized to the surface of each biosensor for 3 min, followed by a 1 min equilibration. A 30 µg/mL aliquot of SRK-015, GDF8_090, SR8-C1, GDF8_029, or GDF8_050 was then allowed to associate with the sensor-bound latent myostatin for 10 min. The antibodies were then dissociated in kinetics buffer at either pH 7.4 or 5.0 for 15 min. Dissociation rates were calculated using ForteBio Data Analysis software (version 8.2) by performing a partial fit of only the dissociation step. A ratio of the dissociation at pH 5 to the dissociation at pH 7.4 was calculated for each antibody tested, with a greater positive number indicating a more rapid dissociation in acidic pH.

Analysis of Latent Myostatin by Size Exclusion Chromatography (SEC)

Preparations of latent myostatin were diluted to 50 µg in either a pH 2.0, 4.0, or 7.4 assay buffer and incubated at RT for 2 h. The prepared samples were then injected onto an SEC column (cat. no. 28-9909-45; GE Healthcare, Chicago, IL) on Waters high-performance liquid chromatography (HPLC; cat. no. e2695; Waters, Milford, MA) using the pH 7.4 buffer at a flow rate of 0.5 mL/min.

Collection of Serum Samples from SRK-015-Dosed Cynomolgus Monkeys

Male cynomolgus monkeys were randomized into four groups of six animals per group. Monkeys were dosed once weekly via intravenous (IV) infusions for 8 weeks, followed by a 4-week washout period. Animals were administered either vehicle control or SRK-015 at doses of 3, 10, or 30 mg/kg/week. Serum samples were collected prior to dosing and on days 2, 4, 6, 8, 15, 22, 29, 36, 43, 64, 72, and 85. When the collection days fell on dosing days, the samples were collected prior to dosing. The cynomolgus study was performed in compliance with the Animal Welfare Act, Guide for the Care and Use of Laboratory Animals, and the Office of Laboratory Animal Welfare.

Results

Identifying Antibody Pairs to Detect Latent Myostatin

To identify antibodies for use as assay reagents, a panel comprising both previously described antibodies,[15] discovered from an internal antibody campaign, and commercially available antimyostatin antibodies was evaluated for binding affinity to the three myostatin forms. From this large panel, antibodies were identified that bound either latent myostatin only or pro- and latent myostatin equally (**Fig. 1D**). Based on this preliminary screen, antibody combinations were subsequently tested in sandwich ELISAs, in which they were used in various combinations as capture or detection reagents to assess sensitivity and selectivity toward latent myostatin. Of these combinations, SR8-C1 and GDF8_090 emerged as the capture and detection reagents, respectively, that showed the best combination of both selectivity toward latent myostatin (**Fig. 1D**) and a low limit of quantitation (**Suppl. Fig. 2 and Fig. 2**).

Serum and SRK-015 Tolerance of the Assay

In cynomolgus monkeys, endogenous myostatin is present in circulation in the 1–30 ng/mL range.[38] To accurately establish standards and controls in a suitable matrix, pooled normal cynomolgus monkey serum was depleted of endogenous myostatin by an affinity column with RK22, an antimyostatin antibody that binds all forms of myostatin (**Fig. 1D**).[38] Belgian blue bovine serum, which is naturally devoid of myostatin, was also tested as a surrogate matrix, but the matrix interference was more substantial than with depleted serum (data not shown). Depleting cynomolgus monkey serum resulted in significant reduction of signal, with detectable latent myostatin comparable to buffer only (no latent myostatin; **Suppl. Fig. S3**). This matrix was then used to prepare standards and control samples.

The matrix effect was assessed to establish the MRD for serum samples analyzed in this assay. The standard curve was prepared in matrices containing 0%, 1%, and 10% myostatin-depleted cynomolgus monkey serum (**Fig. 2**). While the standard curves prepared in each matrix were similar (**Fig. 2A**), we noted that the background signal of the 10% serum standard curve was elevated compared with

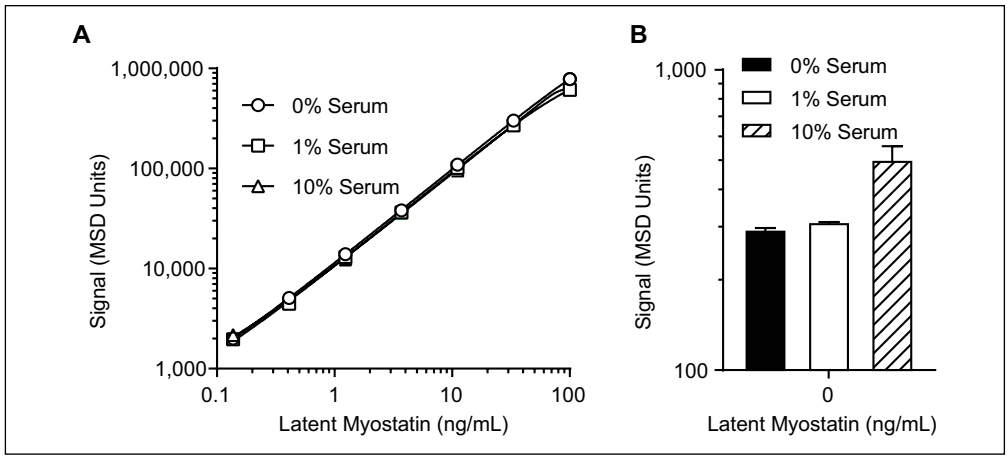

Figure 2. Optimization of the serum concentration and sample diluent pH. (**A**) Similar standard curves are generated from standards prepared in 0%, 1%, or 10% cynomolgus monkey matrix. (**B**) The background signal of the assay, however, shows an increase in signal with 10% serum, while including 1% serum is comparable to buffer alone.

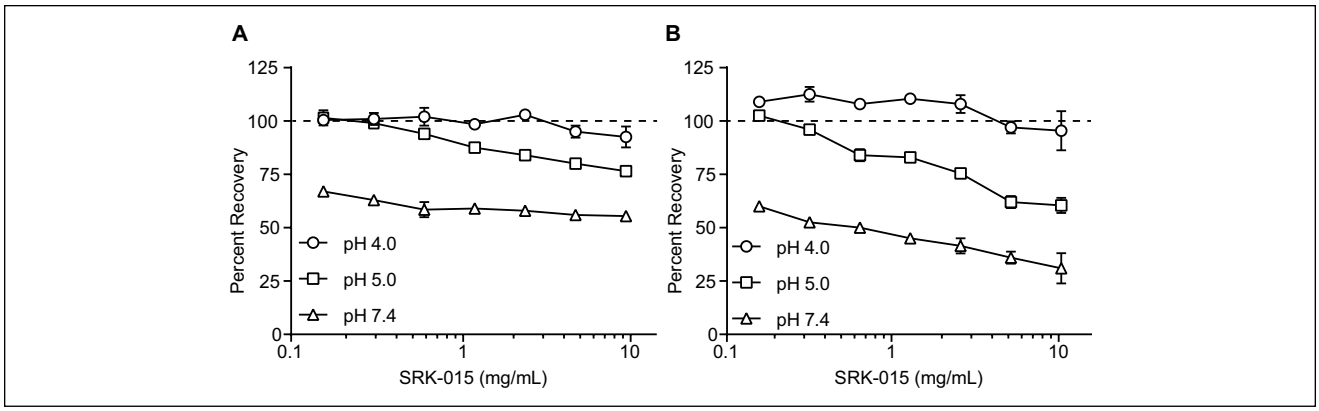

Figure 3. Comparison of assay recovery in the presence of SRK-015 after dilution into sample buffers at pH 4.0, 5.0, and 7.4. Serum samples containing (**A**) 10,000 ng/mL and (**B**) 100 ng/mL of latent myostatin were incubated with varying concentrations of SRK-015. These samples were assayed to calculate the percentage of recovery of the nominal concentration. Accurate quantitation is achieved only when using a sample buffer at pH 4.0.

0% and 1% matrix (**Fig. 2B**). Because of this, the MRD was established at 1:100 to enable sensitive quantitation and minimize the matrix effect.

Next, we assessed the assay's drug tolerance to evaluate it as a potential target engagement assay after dosing with SRK-015. These studies indicated that the assay, as initially designed, was poorly tolerant to the presence of SRK-015 in cynomolgus monkey serum (see the recovery curves at pH 7.4 in **Fig. 3**). During the antimyostatin antibody development, we noted that SRK-015 binding to latent myostatin is pH dependent: The dissociation rate of SRK-015, measured as k_{off} by biolayer interferometry, is approximately 20-fold lower at pH 7.4 than at pH 5.0 (**Suppl. Table S1**). We also tested pH-dependent latent myostatin binding to the assay capture and detection reagents, finding that, like SRK-015, antibody GDF8_090 dissociates from latent myostatin at lower pH (**Suppl. Table S1**). In contrast, the dissociation rate for the SR8-C1–latent myostatin complex could not be determined at pH 5.0 due to a lack of measurable dissociation, suggesting that the SR8-C1–latent myostatin complex is stable at lower pH conditions.

These data suggested that drug tolerance could be improved by diluting SRK-015-treated serum samples in low-pH buffer. To test this, mock samples were prepared with defined amounts of recombinant latent myostatin in the presence of SRK-015. These samples were diluted into buffers at pH 4.0, 5.0, and 7.4, and the percentage of recovery of the controls was calculated in the presence of varying concentrations of SRK-015. Consistent with the finding that SRK-015 does not bind latent myostatin at low pH, tolerance for SRK-015 increases as pH decreases (**Fig. 3**). At pH 4.0, all of the control samples recover to within $\pm$14%, up to the maximum of 10 mg/mL SRK-015 tested. At pH 5.0, the controls can tolerate up to 2.5 mg/mL of SRK-015, while at pH 7.4 the assay tolerance is $<$0.16 mg/mL.

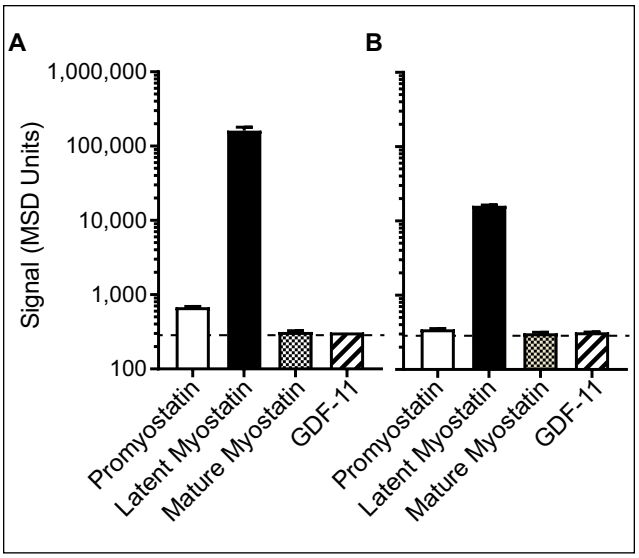

Figure 4. The optimized assay is highly selective toward latent myostatin. After optimization of the assay, each myostatin form and GDF11 were spiked into the assay at (**A**) 10 µg/mL or (**B**) 1 µg/mL, and analyzed for detection. Only latent myostatin shows robust signals in the assay at a high and low concentration.

In vitro incubation of latent myostatin at pH 2.5 has been shown to cause growth factor release.[21] Therefore, to evaluate whether incubation of latent myostatin at pH 4.0 also causes this dissociation, we measured pH-dependent growth factor release. After a 2 h incubation at pH 2.0, 4.0, or 7.4, samples were separated by SEC. As shown in **Supplemental Figure 4**, there is little change in the distribution and size of the peaks after incubation at pH 7.4 or 4.0. In contrast, a high-molecular-weight aggregate is detected after incubation at pH 2.0, as well as a shift in the major peak and a shoulder off of the main peak. The retention times of the new peaks are consistent with the fully proteolyzed portions of latent myostatin.[39] These data indicate that incubation of latent myostatin at pH 4.0 does not cause growth factor release, suggesting that such treatment is a viable method for reducing SRK-015 drug tolerance in this assay without concomitantly affecting the analyte.

Finally, binding to pro-, latent, and mature myostatin was reassessed to ensure that the assay retains specificity toward latent myostatin at pH 4.0. Each myostatin form was spiked into the assay at 10 µg/mL (**Fig. 4A**) or 1 µg/mL (**Fig. 4B**), and, in each case, only the signal from latent myostatin was detected.

Serum Latent Myostatin Assay Qualification

To establish robustness and reproducibility, the assay was qualified using best practices,[33,34] with the following acceptance criteria: recovery within 75–125% of the nominal concentration, a CV percentage (%CV) lower than 25%, and the total error (deviation from 100% recovery plus the %CV) lower than 30%. Accuracy and precision were calculated by assaying five control samples across six plates throughout 3 days. **Table 1** shows the cumulative data for these controls. Quality controls (QCs) consistently met acceptance criteria both within each plate and averaged among all plates, indicating that the assay achieves acceptable accuracy and precision. The LLOQ was established at 10 ng/mL and was established by the above acceptance criteria, and it gave a signal approximately twofold greater than the background signal.

Dilutional linearity was tested by diluting a mock sample containing 4 mg/mL latent myostatin to the MRD and beyond to assess assay precision among a range of dilutions (**Table 1**). Because this control needed to be diluted at least 1:240 to fall lower than the ULOQ (upper limit of quantitation) of the assay (16.7 µg/mL), the 1:100 dilution was above the limit of quantitation (ALQ). All of the remaining diluted samples, however, recovered to within ±20% of the nominal concentration (total error within ± 30%). These data indicate that samples containing neat latent myostatin concentrations higher than the assay's ULOQ can be accurately measured after dilution.

Finally, to assess serum latent myostatin stability during sample handling and analysis, high and low controls were incubated at temperatures and times mirroring common sample storage conditions. In addition, control samples were subjected to five freeze–thaw cycles to assess freeze–thaw stability. All samples subjected to these conditions yielded accurate results as measured by the percentage of recovery of the controls (**Table 1**).

Analysis of Cynomolgus Monkey Serum Samples

To evaluate changes in latent myostatin in SRK-015-dosed nonhuman primates, we analyzed samples from a repeat-dose pharmacology study in cynomolgus monkeys. Animals were assigned to one of four cohorts and were dosed with 0 (vehicle control), 3, 10, or 30 mg/kg/week of SRK-015 for a total of eight doses. Latent myostatin was measured in serum samples collected at regular intervals throughout the study, including samples from a washout period in which SRK-015 dosing was stopped but collection of serum samples continued. **Figure 5** shows the group-averaged latent myostatin concentrations throughout the course of the study, and **Supplemental Figure 5** shows the individual curves. After SRK-015 treatment, latent myostatin rapidly accumulated in serum and plateaued after additional weekly doses, suggesting full saturation of the target. This accumulation trended back toward baseline during the washout period, particularly in the low-dose cohort. While this effect was not statistically significant, it suggests that the accumulation of latent myostatin may be reversed as the drug is cleared from circulation.

Table 1. Control Performance across Various Conditions.

	Control	Nominal (ng/mL)	Calculated Concentration (ng/mL)	%CV	Recovery (%)	Total Error (%)
Assay	ULOQ	16,670	16,130	14	97	17
Reproducibility QCs	HQC	10,000	10,410	13	104	17
	MQC	1000	980	13	98	15
	LQC	100	93	14	94	20
	LLOQ	10	10	12	104	16
	Negative	0	0	N/A	N/A	N/A
Dilutional Linearity QCs	1:100	40,000	ALQ	N/A	ALQ	N/A
	1:250	16,000	18,348	8	115	23
	1:500	8000	9467	11	118	29
	1:1000	4000	4453	10	111	21
Stability QCs	Freeze–thaw HQC	10,000	9871	15	99	16
	Freeze–thaw LQC	100	100	5	100	5
	Room temp HQC	10,000	9272	6	93	13
	Room temp LQC	100	94	3	93	10
	2–8 °C HQC	10,000	10,351	4	104	8
	2–8 °C LQC	100	103	3	103	6

Each control sample was spiked in the assay at 1:100 or further, and assayed for accuracy and precision. ALQ, Above the limit of quantitation; %CV, percentage of coefficient of variation; HQC, higher quality control; LLOC, lower limit of quantitation; LQC, lower quality control; MQC, medium quality control; N/A, not available; QC, quality control; ULOC, upper limit of quantitation.

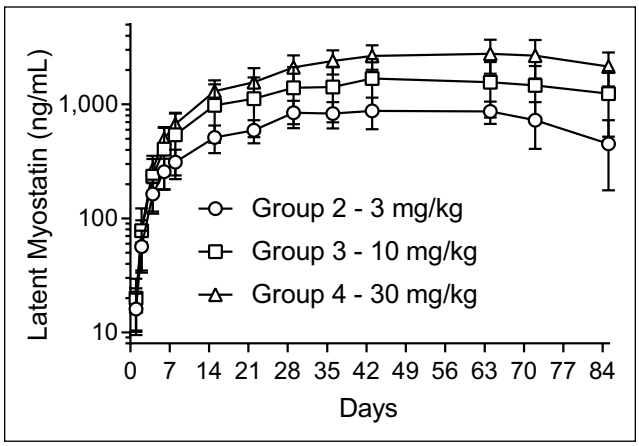

Figure 5. Group-averaged latent myostatin concentration (reported as mean and percentage of coefficient of variation, $n = 6$). Cynomolgus monkeys were dosed with SRK-015 weekly for a total of eight doses. Serum samples were collected throughout the dosing phase and through a 4-week washout period. There is a dose-dependent (but not dose-proportional) response to the amount of accumulated latent myostatin. After the last dose, latent myostatin trends back toward baseline.

Discussion

Here, we describe a plate-based bioassay that selectively detects latent myostatin, the most abundant form of myostatin in circulation.[15] Prior to development of this assay, methods for directly measuring specific myostatin proforms in biological samples were limited to mass spectrometry–based technologies.[29–32] While mass spectrometry has become more accessible, ELISAs and plate-based immmunoassays offer higher throughput and lower cost, and they pose fewer technical challenges. Furthermore, unlike established myostatin ELISAs that require conversion of all myostatin forms to the mature form prior to analysis,[21–26] the assay described here directly measures latent myostatin, thereby reducing the sample manipulation required.

A major challenge in developing a latent myostatin–specific assay lay in identifying reagents that distinguished between the myostatin growth factor and its two proforms. We achieved such specificity through the combined selectivity of two assay reagents: the antibody GDF8_090, which specifically binds the prodomain of both the pro- and latent forms of myostatin, and SR8-C1, which binds to the mature growth factor either in its released form or in the context of the latent myostatin form. Used together in an ELISA format, these antibodies provide excellent specificity for latent myostatin (**Fig. 1D and Fig. 4**).

To optimize the assay drug tolerance, a pH 4.0 sample buffer was used to dissociate SRK-015 from latent myostatin. A typical acid dissociation step, often used in anti-drug antibody assays, would dissociate the antibody–antigen complex at very low pH (1.5–2.0). Because the mature myostatin growth factor is released from the complex at pH $\leq$2, however, such dissociation risks significantly altering the analyte, converting any latent myostatin into the mature form (**Suppl. Fig. S4**). By incubating samples at pH 4.0, we

successfully dissociate SRK-015 from latent myostatin while leaving the analyte intact, enabling a drug-tolerant plate-based immunoassay that sensitively and selectively quantifies total latent myostatin levels in SRK-015-treated cynomolgus monkey serum.

Circulating myostatin levels have been proposed as a biomarker for muscle-wasting diseases, including sarcopenia and cachexia.[40–43] Mass spectrometry–based assays indicate that the circulating level of myostatin in healthy humans is in the 5–10 ng/mL range, depending on age and gender,[29–32] with similar levels in cynomolgus monkeys.[38] The LLOQ of our latent myostatin assay is 10 ng/mL (**Table 1**), suggesting that the current form of the assay is insufficiently sensitive for assessing latent myostatin as a biomarker in untreated monkey or human serum. Basal levels of circulating latent myostatin in mice are, however, significantly higher: in the 100–300 ng/mL range, much higher than the LLOQ for this assay. We are therefore using our ELISA to evaluate latent myostatin as a disease biomarker in mice, and preliminary studies suggest a measurable difference between basal latent myostatin levels in normal mice and those with a spinal muscular atrophy (SMA) phenotype.[16] Thus, while our primary goal was to measure accumulation of circulating target after SRK-015 dosing, the LLOQ of the assay suggests potential utility in measuring latent myostatin as a predictive biomarker. Further efforts to increase the sensitivity to support this aim will be guided by preclinical studies.

Finally, although serum data are a useful measure of target engagement, it is important to note that myostatin functions within the muscle.[1] While we assume that target engagement in serum directly relates to engagement in muscle, we have not yet shown a direct relationship between the extent of target engagement and increased muscle hypertrophy. The assay described here, which is capable of discriminating specific pro- forms of myostatin in serum, suggests that a similar approach could be taken to measure pro- and latent myostatin in samples from muscle biopsies. This would allow accurate pro- and latent myostatin quantitation in disease states or after dosing with SRK-015, providing greater insight into the biology of myostatin processing and the relationship between circulating and muscle myostatin levels as they relate to muscle hypertrophy.

Acknowledgments

The authors acknowledge Alan Buckler and Ryan Faucette for their contributions to the review of this manuscript.

Declaration of Conflicting Interests

The authors disclosed the following potential conflicts of interest with respect to the research, authorship, and/or publication of this article: All authors were employed by Scholar Rock, Inc. at the time of the work on the article and their research and authorship of this article was completed within the scope of this employment.

Funding

The authors received no financial support for the research, authorship, and/or publication of this article.

ORCID iD

Shaun M. Cote https://orcid.org/0000-0003-4596-9301

References

1. Anderson, S. B.; Goldberg, A. L.; Whitman, M. Identification of a Novel Pool of Extracellular Pro-Myostatin in Skeletal Muscle. *J. Biol. Chem*. **2008**, *283*, 7027–7035.
2. McPherron, A. C.; Lawler, A. M.; Lee, S.-J. Regulation of Skeletal Muscle Mass in Mice by a New TGF-β Superfamily Member. *Nature*. **1997**, *387*, 83–90.
3. Rodgers, B. D.; Interlichia, J. P.; Garikipati, D. K.; et al. Myostatin Represses Physiological Hypertrophy of the Heart and Excitation–Contraction Coupling. *J. Physiol*. **2009**, *587*, 4873–4886.
4. Grobet, L.; Royo Martin, L. J.; Poncelet, D.; et al. A Deletion in the Bovine Myostatin Gene Causes the Double–Muscled Phenotype in Cattle. *Nat. Genet*. **1997**, *17*, 71–74.
5. Kambadur, R.; Sharma, M.; Smith, T. P. L.; et al. Mutations in Myostatin (GDF8) in Double-Muscled Belgian Blue and Piedmontese Cattle. *Genome Res*. **1997**, *7*, 910–915.
6. Mosher, D. S.; Quignon, P.; Bustamante, C. D.; et al. A Mutation in the Myostatin Gene Increases Muscle Mass and Enhances Racing Performance in Heterozygote Dogs. *PLoS Genet*. **2007**, *3*, e79.
7. Schuelke, M.; Wagner, K. R.; Stolz, L. E.; et al. Myostatin Mutation Associated with Gross Muscle Hypertrophy in a Child. *N. Engl. J. Med*. **2004**, *350*, 2682–2688.
8. McPherron, A. C.; Lee, S.-J. Double Muscling in Cattle Due to Mutations in the Myostatin Gene. *Proc. Natl. Acad. Sci. USA*. **1997**, *94*, 12457–12461.
9. Varga, L.; Müller, G.; Szabó, G.; et al. Mapping Modifiers Affecting Muscularity of the Myostatin Mutant (MstnCmpt-Dl1Abc) Compact Mouse. *Genetics*. **2003**, *165*, 257–267.
10. Zimmers, T. A.; Davies, M. V.; Koniaris, L. G.; et al. Induction of Cachexia in Mice by Systemically Administered Myostatin. *Science*. **2002**, *296*, 1486–1488.
11. Latres, E.; Pangilinan, J.; Miloscio, L.; et al. Myostatin Blockade with a Fully Human Monoclonal Antibody Induces Muscle Hypertrophy and Reverses Muscle Atrophy in Young and Aged Mice. *Skelet. Muscle*. **2015**, *5*, 34.
12. Padhi, D.; Higano, C. S.; Shore, N. D.; et al. Pharmacological Inhibition of Myostatin and Changes in Lean Body Mass and Lower Extremity Muscle Size in Patients Receiving Androgen Deprivation Therapy for Prostate Cancer. *J. Clin. Endocrinol. Metab*. **2014**, *99*, E1967–E1975.
13. Zhang, L.; Rajan, V.; Lin, E.; et al. Pharmacological Inhibition of Myostatin Suppresses Systemic Inflammation and Muscle Atrophy in Mice with Chronic Kidney Disease. *FASEB J*. **2011**, *25*, 1653–1663.

14. Becker, C.; Lord, S. R.; Studenski, S. A.; et al. Myostatin Antibody (LY2495655) in Older Weak Fallers: A Proof-of-Concept, Randomised, Phase 2 Trial. *Lancet Diabetes Endocrinol*. **2015**, *3*, 948–957.
15. Pirruccello-Straub, M.; Jackson, J.; Wawersik, S.; et al. Blocking Extracellular Activation of Myostatin as a Strategy for Treating Muscle Wasting. *Sci. Rep*. **2018**, *8*, 2292.
16. Long, K. K.; O'Shea, K. M.; Khairallah, R. J.; et al. Specific Inhibition of Myostatin Activation Is Beneficial in Mouse Models of SMA Therapy. *Hum. Mol. Genet*. **2018**, *28*, 1076–1089.
17. Glanzman, A. M.; O'Hagen, J. M.; McDermott, M. P.; et al. Validation of the Expanded Hammersmith Functional Motor Scale in Spinal Muscular Atrophy Type II and III. *J. Child Neurol*. **2011**, *26*, 1499–1507.
18. O'Hagen, J. M.; Glanzman, A. M.; McDermott, M. P.; et al. An Expanded Version of the Hammersmith Functional Motor Scale for SMA II and III Patients. *Neuromuscul. Disord*. **2007**, *17*, 693–697.
19. Ramsey, D.; Scoto, M.; Mayhew, A.; et al. Revised Hammersmith Scale for Spinal Muscular Atrophy: A SMA Specific Clinical Outcome Assessment Tool. *PLoS One*. **2017**, *12*, e0172346.
20. Mazzone, E. S.; Mayhew, A.; Montes, J.; et al. Revised Upper Limb Module for Spinal Muscular Atrophy: Development of a New Module. *Muscle Nerve*. **2017**, *55*, 869–874.
21. Lakshman, K. M.; Bhasin, S.; Corcoran, C.; et al. Measurement of Myostatin Concentrations in Human Serum: Circulating Concentrations in Young and Older Men and Effects of Testosterone Administration. *Mol. Cell. Endocrinol*. **2009**, *302*, 26–32.
22. Han, D.-S.; Chu-Su, Y.; Chiang, C.-K.; et al. Serum Myostatin Is Reduced in Individuals with Metabolic Syndrome. *PLoS One*. **2014**, *9*, e108230.
23. Invernizzi, M.; Carda, S.; Rizzi, M.; et al. Evaluation of Serum Myostatin and Sclerostin Levels in Chronic Spinal Cord Injured Patients. *Spinal Cord*. **2015**, *53*, 615–620.
24. Wintgens, K. F.; Dschietzig, T.; Stoeva, S.; et al. Plasma Myostatin Measured by a Competitive ELISA Using a Highly Specific Antiserum. *Clin. Chim. Acta*. **2012**, *413*, 1288–1294.
25. Han, D. S.; Chen, Y. M.; Lin, S. Y.; et al. Serum Myostatin Levels and Grip Strength in Normal Subjects and Patients on Maintenance Haemodialysis. *Clin. Endocrinol. (Oxf.)*. **2011**, *75*, 857–863.
26. Diel, P.; Schiffer, T.; Geisler, S.; et al. Analysis of the Effects of Androgens and Training on Myostatin Propeptide and Follistatin Concentrations in Blood and Skeletal Muscle Using Highly Sensitive Immuno PCR. *Mol. Cell. Endocrinol*. **2010**, *330*, 1–9.
27. Khalil, A. M.; Dotimas, H.; Kahn, J.; et al. Differential Binding Activity of TGF-β Family Proteins to Select TGF-β Receptors. *J. Pharmacol. Exp. Ther*. **2016**, *358*, 423–430.
28. Padyana, A. K.; Vaidialingam, B.; Hayes, D. B.; et al. Crystal Structure of Human GDF11. *Acta Crystallogr. Sect. F Struct. Biol. Commun*. **2016**, *72*, 160–164.
29. Bergen, H. R.; Farr, J. N.; Vanderboom, P. M.; et al. Myostatin as a Mediator of Sarcopenia versus Homeostatic Regulator of Muscle Mass: Insights Using a New Mass Spectrometry-Based Assay. *Skelet. Muscle*. **2015**, *5*, 21.
30. Palandra, J.; Quazi, A.; Fitz, L.; et al. Quantitative Measurements of GDF-8 Using Immunoaffinity LC-MS/MS. *Proteomics Clin. Appl*. **2016**, *10*, 597–604.
31. Zhu, Y.; D'Arienzo, C.; Lou, Z.; et al. LC–MS/MS Multiplexed Assay for the Quantitation of a Therapeutic Protein BMS-986089 and the Target Protein Myostatin. *Bioanalysis*. **2016**, *8*, 193–204.
32. Peiris, H. N.; Ashman, K.; Vaswani, K.; et al. Method Development for the Detection of Human Myostatin by High-Resolution and Targeted Mass Spectrometry. *J. Proteome Res*. **2014**, *13*, 3802–3809.
33. Cummings, J.; Raynaud, F.; Jones, L.; et al. Fit-for-Purpose Biomarker Method Validation for Application in Clinical Trials of Anticancer Drugs. *Br. J. Cancer*. **2010**, *103*, 1313–1317.
34. US Food and Drug Administration (FDA). *Bioanalytical Method Validation (Guidance for Industry)*. US Department of Health and Human Services, FDA, Center for Drug Evaluation and Research: Rockville, MD, 2018, p. 44.
35. Recommended INN: List 75: Trevogrumab. *WHO Drug Inf*. **2016**, *30*, 160–161.
36. LaVallie, E. R.; Collins-Racie, L. A.; Corcoran, C. J.; et al. Antibody to GDF8 and Uses Thereof. US Patent 8,415,459, April 9, **2013**.
37. Recommended INN: List 76: Domagrozumab. *WHO Drug Inf*. **2016**, *30*, 495–496.
38. St. Andre, M.; Johnson, M.; Bansal, P. N.; et al. A Mouse Anti-Myostatin Antibody Increases Muscle Mass and Improves Muscle Strength and Contractility in the Mdx Mouse Model of Duchenne Muscular Dystrophy and Its Humanized Equivalent, Domagrozumab (PF-06252616), Increases Muscle Volume in Cynomolgus Monkeys. *Skelet. Muscle*. **2017**, *7*.
39. Le, V. Q.; Iacob, R. E.; Tian, Y.; et al. Tolloid Cleavage Activates Latent GDF8 by Priming the Pro-Complex for Dissociation. *EMBO J*. **2018**, *37*, 384–397.
40. Scharf, G.; Heineke, J. Finding Good Biomarkers for Sarcopenia. *J. Cachexia Sarcopenia Muscle*. **2012**, *3*, 145–148.
41. Kalinkovich, A.; Livshits, G. Sarcopenia—The Search for Emerging Biomarkers. *Ageing Res. Rev*. **2015**, *22*, 58–71.
42. Cavalier, E.; Beaudart, C.; Buckinx, F.; et al. Critical Analytical Evaluation of Promising Markers for Sarcopenia. *Eur. Geriatr. Med*. **2016**, *7*, 239–242.
43. Drescher, C.; Konishi, M.; Ebner, N.; et al. Loss of Muscle Mass: Current Developments in Cachexia and Sarcopenia Focused on Biomarkers and Treatment: Loss of Muscle Mass: Current Developments. *J. Cachexia Sarcopenia Muscle*. **2015**, *6*, 303–311.